Robotica (2010) volume 28, pp. 821–832. © Cambridge University Press 2009
doi:10.1017/S0263574709990683

On the kinematics of the 3-RRUR spherical parallel manipulator

R. Deidda, A. Mariani and M. Ruggiu*

Department of Mechanical Engineering, University of Cagliari, Piazza d'Armi - 09123 Cagliari, Italy

(Received in Final Form: April 22, 2009. First published online: December 7, 2009)

SUMMARY

In the present paper, the kinematics of a three-degree-of-freedom spherical wrist is investigated. The wrist consists of a fixed base connected to a moving platform by three identical legs, each with a RRUR chain (R and U denote a revolute pair and a universal pair, respectively). For each leg, the first R pair is to be considered actuated. Although in previous works the kinematics synthesis of this architecture was carried out, no detailed studies were presented on the kinematic issues of the wrist. This paper presents the mobility analysis, the direct and inverse position kinematics, the differential kinematics of the manipulator including inspection on the jacobian matrix and the analysis of the singularities. The geometrical condition matched in case of mechanical interference between legs is addressed, too. A numerical example of the manipulator kinematics was performed to obtain the workspace, the condition number and the mechanical inteference condition.

KEYWORDS: Spherical parallel manipulators; Orienting devices; Robotic wrist.

1. Introduction

Spherical parallel mechanisms (SPMs) refer to three degree-of-freedom (DOF) manipulators in which the moving platform rotates about a fixed point designated as the center of spherical motion. This type of mechanism may find numerous applications including orientating devices or wrists exploiting some advantages of a parallel architecture over a serial architecture: accuracy and repeatability of positioning, likely due to high structural stiffness of the mechanism, and excellent dynamic properties. Numerous SPMs with three independent legs (tripods) have been proposed. A rough classification may be devised by considering either overconstrained or not overconstrained architectures. The best-known overconstrained architecture is the 3-RRR proposed by Gosselin *et al.*[1–5] To assure the spherical motion of the moving platform, all the axes of the mechanism must converge into the center of spherical motion. It is well known, however, that some technological drawbacks may arise because of the great accuracy required in the technological process. For that reason, just as many not-overconstrained wrists have also been devised. The not-overconstrained architecture is typically a tripod with each leg having five DOFs (connectivity five).[6, 7] Some examples of not-overconstrained wrists are the 3-RRS (S stands for a spherical pair), the 3-RUU, and the 3-UCR (C stands for a cylindrical pair) architectures.[8–10] Both the 3-RRS and 3-RUU exhibit simple architectures employing just two links for each leg; furthermore, the 3-RUU uses only revolute pairs, thus allowing for an easier technological process. The above-mentioned architectures are the result of the great effort that some researchers have made to propose methods of synthesis for SPMs. While Kong and Gosselin adopted the screw theory,[11–13] Karouia and Hervè formalized an approach of synthesis that takes advantage of the algebraic structure of the Lie group.[6, 7] Both the researchers groups formalized the synthesis of the 3-RRUR architecture as a spherical manipulator which is the subject of this paper. Because of the potential applications of the 3-RRUR (i.e., orientation wrist for cameras, sensors, medical devices, haptic interfaces) and since no detailed studies on its kinematics were found, the present paper proposes the full kinematic analysis of the wrist.

The paper is structured as follows: In Section 2 the geometry of the manipulator and the proof of the spherical motion of the moving platform by differential kinematics are presented. In Section 3 the formulation of the kinematic equations is given. Sections 4 and 5 provide the analytical solution of the inverse and direct position kinematics, respectively. In Section 6 a numerical example of workspace calculation is provided. Section 7 deals with the differential kinematics to obtain an analytical form of the jacobian. In Section 8 inspection on the jacobian allowed us to detect the singularities of this manipulator. Furthermore, in this section the numerical example of Section 6 is re-proposed to calculate the condition number. Section 9 provides the geometrical condition matched in case of mechanical interference between the legs of the wrist. Finally, the conclusions are drawn.

2. Geometry of the Manipulator and Mobility Analysis

According to Kong *et al.*,[13] there are 16 types of spherical tripods involving only R pairs and with connectivity 5 for each leg (not-overconstrained). Amongst them only tripods with each leg constituted by a kinematic chain equivalent to a planar joint and two R pairs whose axes intersect was selected. The use of the equivalent planar joint instead of the equivalent spherical joint, i.e., $3R \equiv S$, simplify the assembling issues. In that case, indeed, for each leg, the two R pairs should intersect as well as the axes of the equivalent spherical joint. Besides, it was decided that the equivalent planar joint was formed only by R pairs in

* Corresponding author. E-mail: ruggiu@dimeca.unica.it

https://doi.org/10.1017/S0263574709990683 Published online by Cambridge University Press

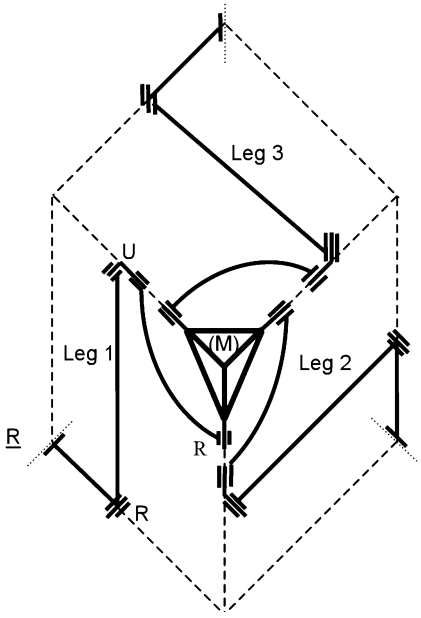


Fig. 1. The 3-RRUR spherical parallel manipulator.

order to avoid friction phenomena and inaccuracies of the P pairs. In addition, the equivalent planar pair was placed at the beginning of the leg. In so doing the intersection of the axes of the two R joints of each leg coincide with the center of the spherical motion of the moving platform. The kinematic analysis of such type of tripods looks simple since the analysis can exploit *the planar nature of each leg* and *the intersecting condition of their two R joints axes*.

Figure 1 illustrates the 3-RRUR. The manipulator consists of a fixed base and a moving platform (M) connected to each other by three legs, each with a RRUR kinematic chain. The R pairs connected to the frame are to be considered actuated.

As can be observed in Fig. 1, at the nominal pose (zero rotation of the moving platform), each manipulator's leg belongs to a face of a cube, i.e., the nominal cube. From Fig. 1 it can be seen that the actuated R pairs coincide with three vertices of the nominal cube and that, due to the symmetry, the moving platform is a tetrahedron. The following reference frames are defined in studying the kinematics of the manipulator (Fig. 2). A fixed reference frame $OX_0Y_0Z_0$, hereafter {0}, with origin O coincident with a vertex of the nominal cube and axes which are pointing along the edges of the nominal cube. A reference frame $PX_GY_GZ_G$, hereafter {G}, attached to the moving platform and with P coincident with a vertex of the tetrahedron. At the nominal pose the rotation matrix of {G} with respect to {0}, hereafter ${}^0\mathbf{R}_G$, coincides with the identity matrix $\mathbf{I}$. For each leg a fixed reference frame {Ji} is determined which has its axis $\mathbf{x}_{Ji}$ pointing along the axis of the R pair connected to the frame. Depending on which leg is considered, the rotation matrix ${}^0\mathbf{R}_{Ji}$ takes different forms such that

$$\begin{aligned} Leg1 &: {}^0\mathbf{R}_{J1} = \mathbf{I}, \\ Leg2 &: {}^0\mathbf{R}_{J2} = \mathbf{R}_{z_0}(\pi/2), \\ Leg3 &: {}^0\mathbf{R}_{J3} = \mathbf{R}_{x_0}(\pi/2)\mathbf{R}_{z_0}(-\pi/2). \end{aligned} \tag{1}$$

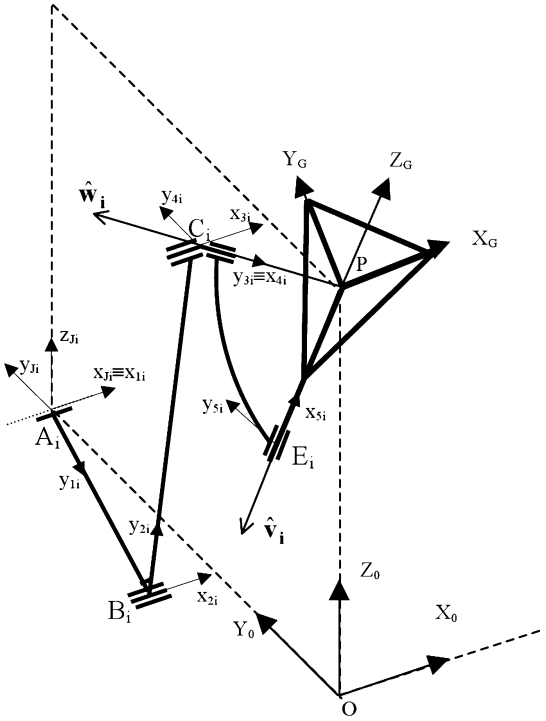


Fig. 2. The reference frames for the analysis of the kinematics.

$\mathbf{R}_{x_0}$, $\mathbf{R}_{z_0}$ denote the basic rotation matrices about the $\mathbf{x}_0$ and $\mathbf{z}_0$ axes, respectively. Traversing the ith leg the $x_{ji}y_{ji}z_{ji}$ $(j = 1, \ldots, 5)$ local reference frames are defined with $\mathbf{x}_{ji}$ pointing along the axis of the jth R pair. $\vartheta_{ji}\mathbf{x}_{ji}$ denotes the rotation of the jth with respect to the $(j-1)$th reference frame, except for $\vartheta_{1i}\mathbf{x}_{1i}$ which locates the first reference frame with respect to the fixed reference frame {Ji}.

With reference to Fig. 2 we define the following vectors:

$$\begin{aligned} \mathbf{a}_i &= \mathbf{A}_i\mathbf{B}_i, & a &= |\mathbf{a}_i|, \\ \mathbf{b}_i &= \mathbf{B}_i\mathbf{C}_i, & b &= |\mathbf{b}_i|, \\ \mathbf{d}_i &= \mathbf{C}_i\mathbf{P}, & d &= |\mathbf{d}_i|, \\ \mathbf{h}_i &= \mathbf{E}_i\mathbf{P}, & h &= |\mathbf{h}_i|, \\ \hat{\mathbf{v}}_i &= -\frac{\mathbf{h}_i}{h}, \\ \hat{\mathbf{w}}_i &= -\frac{\mathbf{d}_i}{d}, \end{aligned} \tag{2}$$

where notation $\mathbf{Q}_i\mathbf{T}_i$ indicates a vector with direction from Q_i to T_i, $|\mathbf{u}|$ indicates the length of vector $\mathbf{u}$ and $\hat{\mathbf{u}}$ is the unit $\mathbf{u}$ vector. From the geometry of the manipulator it follows that $a + d = b$, which is the length of the nominal cube edge.

The synthesis of the architecture being studied as a spherical manipulator is due to the exhaustive work of Hervè and Karouia[6, 7] who proved that the 3-RRUR is a SPM by displacement Lie group algebra and by Kong and Gosselin[11–13] who worked with screw–wrench systems.

An alternative proof may be carried out by differential kinematics (Fig. 2). The velocity of point P can be written

https://doi.org/10.1017/S0263574709990683 Published online by Cambridge University Press

as

$$\mathbf{v}_P = \dot{\vartheta}_{1i}\mathbf{x}_{1i} \times \mathbf{a}_i + \sum_{j=1}^{2} \dot{\vartheta}_{ji}\mathbf{x}_{1i} \times \mathbf{b}_i + \left[\sum_{j=1}^{3} \dot{\vartheta}_{ji}\mathbf{x}_{1i} + \dot{\vartheta}_{4i}\mathbf{x}_{4i}\right] \times (\mathbf{d}_i - \mathbf{h}_i) + \left[\sum_{j=1}^{3} \dot{\vartheta}_{ji}\mathbf{x}_{1i} + \dot{\vartheta}_{4i}\mathbf{x}_{4i} + \dot{\vartheta}_{5i}\mathbf{x}_{5i}\right] \times \mathbf{h}_i, \quad (3)$$

where all vectors are expressed in {0} (no leading superscript).

Considering that $\mathbf{x}_{4i} \times \mathbf{d}_i = \mathbf{x}_{5i} \times \mathbf{h}_i = 0$, after simple manipulations we obtain

$$\mathbf{v}_P = \dot{\vartheta}_{1i}\mathbf{x}_{1i} \times \mathbf{s}_i + \dot{\vartheta}_{2i}\mathbf{x}_{1i} \times \mathbf{l}_i + \dot{\vartheta}_{3i}\mathbf{x}_{1i} \times \mathbf{d}_i, \quad (4)$$

where

$$\mathbf{s}_i = \mathbf{a}_i + \mathbf{b}_i + \mathbf{d}_i\,, \mathbf{l}_i = \mathbf{b}_i + \mathbf{d}_i. \quad (5)$$

Dot multiplying by $\mathbf{x}_{1i}$ both sides of Eq. (4) and observing that $\mathbf{x}_{1i}$ is perpendicular to $\mathbf{s}_i$, $\mathbf{l}_i$ and $\mathbf{d}_i$:

$$\mathbf{v}_P \cdot \mathbf{x}_{1i} = \dot{\vartheta}_{1i}\mathbf{x}_{1i} \times \mathbf{s}_i \cdot \mathbf{x}_{1i} + \dot{\vartheta}_{2i}\mathbf{x}_{1i} \times \mathbf{l}_i \cdot \mathbf{x}_{1i} + \dot{\vartheta}_{3i}\mathbf{x}_{1i} \times \mathbf{d}_i \cdot \mathbf{x}_{1i} = 0. \quad (6)$$

Equation (6) can be differentiated with respect to the time:

$$\dot{\mathbf{v}}_P \cdot \mathbf{x}_{1i} + \mathbf{v}_P \cdot \dot{\mathbf{x}}_{1i} = \dot{\mathbf{v}}_P \cdot \mathbf{x}_{1i} = 0. \quad (7)$$

Since $\mathbf{x}_{1i}$s are fixed. Equations (6) and (7) can be expressed in matrix form:

$$\mathbf{N}\begin{bmatrix}\mathbf{v}_P \\ \dot{\mathbf{v}}_P\end{bmatrix}, \quad (8)$$

where

$$\mathbf{N} = \begin{bmatrix} \mathbf{x}_{11}^T & 0_{1\times3} \\ \mathbf{x}_{12}^T & 0_{1\times3} \\ \mathbf{x}_{13}^T & 0_{1\times3} \\ 0_{1\times3} & \mathbf{x}_{11}^T \\ 0_{1\times3} & \mathbf{x}_{12}^T \\ 0_{1\times3} & \mathbf{x}_{13}^T \end{bmatrix}. \quad (9)$$

$\mathbf{x}_{11}$, $\mathbf{x}_{12}$, and $\mathbf{x}_{13}$ form a vector basis therefore the matrix of coefficient $\mathbf{N}$ has a determinant different from zero. The unique solution of the system of Eq. (8) is $\mathbf{v}_P = \dot{\mathbf{v}}_P = 0$. Therefore P is fixed and the center of the spherical motion of the moving platform.

3. Formulation of the Kinematic Equations

The equations required to solve both the direct and the inverse position kinematics are obtained considering the ith RRUR leg of the manipulator:

$$\mathbf{s}_i = \mathbf{a}_i + \mathbf{b}_i + \mathbf{d}_i, \quad (10)$$

$$\hat{\mathbf{w}}_\mathbf{i} \cdot \hat{\mathbf{v}}_\mathbf{i} = 0. \quad (11)$$

Equation (10) is a loop closure equation with $\mathbf{a}_i$, $\mathbf{b}_i$, $\mathbf{d}_i$ on the same plane (i.e., a face of the nominal cube). It may be noted that $\mathbf{d}_i$ is only a geometrical tool used to facilitate the calculation of the kinematic problems but is not a real link of the leg. Equation (11) exploits the trivial condition that the last two axes of the R pairs in a leg are always perpendicular to one another. Equations (10) and (11) express the nature of each leg of the wrist proposed: the kinematic chain equivalent to a planar joint and two R pairs whose axes intersect.

The explicit formulation of Eq. (10) is

$${}^0\mathbf{R}_{Ji}{}^{Ji}\mathbf{R}_1{}^1\mathbf{a}_i + {}^0\mathbf{R}_{Ji}{}^{Ji}\mathbf{R}_1{}^1\mathbf{R}_2{}^2\mathbf{b}_i + {}^0\mathbf{R}_{Ji}{}^{Ji}\mathbf{R}_1{}^1\mathbf{R}_2{}^2\mathbf{R}_3{}^3\mathbf{d}_i = {}^0\mathbf{R}_{Ji}{}^{Ji}\mathbf{s}_i, (i = 1, 2, 3), \quad (12)$$

where ${}^{(j-1)}\mathbf{R}_j = \mathbf{R}_{x_{ji}}(\vartheta_{ji})$, $j = 1, 2, 3$, and $j - 1 = 0 \equiv Ji$.

Vectors expressed in their own reference frames are

$$\begin{aligned} {}^{\mathbf{1}}\mathbf{a}_\mathbf{i} &= a[0\ 1\ 0]^T, \\ {}^{\mathbf{2}}\mathbf{b}_\mathbf{i} &= b[0\ 1\ 0]^T, \\ {}^{\mathbf{3}}\mathbf{d}_\mathbf{i} &= d[0\ 1\ 0]^T. \end{aligned} \quad (13)$$

${}^{\mathbf{Ji}}\mathbf{s}_\mathbf{i}$ is known by the geometry and depends on the {Ji} reference frame, such that

$$\begin{aligned} Leg1 &: {}^{\mathbf{J1}}\mathbf{s}_\mathbf{1} = [0\ -(a+d)\ b]^T, \\ Leg2 &: {}^{\mathbf{J2}}\mathbf{s}_\mathbf{2} = [0\ b\ (a+d)]^T, \\ Leg3 &: {}^{\mathbf{J3}}\mathbf{s}_\mathbf{3} = [0\ -(a+d)\ b]^T. \end{aligned} \quad (14)$$

For the sake of brevity,

$${}^{\mathbf{0}}\mathbf{s}_\mathbf{i} = {}^0\mathbf{R}_{Ji}{}^{\mathbf{Ji}}\mathbf{s}_\mathbf{i} = [P_{x_i}\ P_{y_i}\ P_{z_i}]^T. \quad (15)$$

Therefore, by simple calculations, the final form of the loop vector equations can be written as

$$\begin{aligned} ac\vartheta_{1i} + bc\vartheta_{1i}\vartheta_{2i} + dc\vartheta_{1i}\vartheta_{2i}\vartheta_{3i} &= P_{y_i}, \\ as\vartheta_{1i} + bs\vartheta_{1i}\vartheta_{2i} + ds\vartheta_{1i}\vartheta_{2i}\vartheta_{3i} &= P_{z_i}. \end{aligned} \quad (16)$$

In Eqs. (16), for the sake of brevity, $\vartheta_{1i}\vartheta_{2i} = (\vartheta_{1i} + \vartheta_{2i})$ and $\vartheta_{1i}\vartheta_{2i}\vartheta_{3i} = (\vartheta_{1i} + \vartheta_{2i} + \vartheta_{3i})$, c($\angle$) and s($\angle$) indicate cos($\angle$) and sin($\angle$), respectively.

Similarly, Eq. (11) can be expressed as

$$\left({}^0\mathbf{R}_3{}^3\hat{\mathbf{w}}_i\right) \cdot \left({}^0\mathbf{R}_G{}^G\hat{\mathbf{v}}_i\right) = \left({}^0\mathbf{R}_{Ji}{}^{Ji}\mathbf{R}_1{}^1\mathbf{R}_2{}^2\mathbf{R}_3{}^3\hat{\mathbf{w}}_i\right) \cdot \left({}^0\mathbf{R}_G{}^G\hat{\mathbf{v}}_i\right) \quad (17)$$

with

$$\begin{aligned} {}^G\hat{\mathbf{v}}_1 &= [0\ 0\ -1]^T, \\ {}^G\hat{\mathbf{v}}_2 &= [1\ 0\ 0]^T, \\ {}^G\hat{\mathbf{v}}_3 &= [0\ 1\ 0]^T, \\ {}^3\hat{\mathbf{w}}_i &= [0\ -1\ 0]^T, \end{aligned} \quad (18)$$

https://doi.org/10.1017/S0263574709990683 Published online by Cambridge University Press

As mentioned, ${}^0\mathbf{R}_G$ is the rotation matrix defining the moving platform orientation with respect to the frame and which contains the Euler's angles of the moving platform. Expanding Eq. (17) for each leg provides:

$$\begin{aligned} &Leg1: r_{23}c\vartheta_{1i}\vartheta_{2i}\vartheta_{3i} + r_{33}s\vartheta_{1i}\vartheta_{2i}\vartheta_{3i} = 0,\\ &Leg2: r_{11}c\vartheta_{1i}\vartheta_{2i}\vartheta_{3i} - r_{31}s\vartheta_{1i}\vartheta_{2i}\vartheta_{3i} = 0,\\ &Leg3: -r_{12}c\vartheta_{1i}\vartheta_{2i}\vartheta_{3i} + r_{22}s\vartheta_{1i}\vartheta_{2i}\vartheta_{3i} = 0, \end{aligned} \tag{19}$$

where r_{ij} is the term of ${}^0\mathbf{R}_G$ at the ith row and at the ith column. Thus, Eqs. (16) and (19) provide nine nonlinear equations with twelve unknowns: ϑ_{1i} ,ϑ_{2i} ,ϑ_{3i} (i = 1, 2, 3), and three Euler's angles ϕ, γ, ψ. Equations (16) and (19) allow for the analytical solution of the position kinematics.

4. Inverse Kinematics

In the inverse position kinematics the Euler's angles ϕ, γ, ψ of the moving platform are given, whilst the actuated rotations ϑ_{1i} (i = 1, 2, 3) are to be calculated. Equations (16) and (19) become nine equations with nine unknowns and they can rewritten in a compact form:

$$ac\mu_i + bc\chi_i + dc\lambda_i = P_{y_i}, \tag{20}$$

$$as\mu_i + bs\chi_i + ds\lambda_i = P_{z_i},$$

$$H_i c\lambda_i + K_i s\lambda_i = 0 \tag{21}$$

with

$$\begin{aligned} \mu_i &= \vartheta_{1i},\\ \chi_i &= \vartheta_{1i}\vartheta_{2i},\\ \lambda_i &= \vartheta_{1i}\vartheta_{2i}\vartheta_{3i},\\ H_1 &= r_{23},\ K_1 = r_{33},\\ H_2 &= r_{11},\ K_2 = -r_{31},\\ H_3 &= -r_{12},\ K_3 = r_{22}. \end{aligned}$$

From Eq. (21),

$${}^{(n=1)}\lambda_i = \text{atan}\frac{-H_i}{K_i}, \tag{22}$$

$${}^{(n=2)}\lambda_i = {}^{(n=1)}\lambda_i + \pi \tag{23}$$

in the range $-\pi \le \lambda_i \le \pi$. Introducing ${}^{(n)}\lambda_i$ in Eq. (21) and separating the unknowns from known terms, these equations can be written as follows:

$${}^{(n)}Y_i = {}^{(n)}P_{yi} - dc({}^{(n)}\lambda_i) = ac({}^{(n)}\mu_i) + bc({}^{(n)}\chi_i) \tag{24}$$

$${}^{(n)}Z_i = {}^{(n)}P_{zi} - ds({}^{(n)}\lambda_i) = as({}^{(n)}\mu_i) + bs({}^{(n)}\chi_i) \tag{25}$$

Equations (24) and (25) look like the inverse kinematic equations of a two link planar manipulator whose algebraic solution was proposed by Craig.[14] We square both Eqs. (24) and (25) and add them, then we use the simple trigonometric relation

$$s({}^{(n)}\chi_i)s({}^{(n)}\mu_i) = c({}^{(n)}\chi_i - {}^{(n)}\mu_i) - c({}^{(n)}\chi_i)c({}^{(n)}\mu_i) \tag{26}$$

to obtain

$${}^{(n)}\vartheta_{2i} = \text{acos}\left[\frac{({}^{(n)}Y_i)^2 + ({}^{(n)}Z_i)^2 - a^2 - b^2}{2ab}\right] \tag{27}$$

Having ${}^{(n)}\vartheta_{2i}$, (n = 1, 2) Eqs. (24) and (25) can be solved for ${}^{(n)}\vartheta_{1i}$. By expanding the terms and collecting the known values, Eqs. (24) and (25) lead to

$${}^{(n)}Y_i = {}^{(n)}k_{1i}c({}^{(n)}\mu_i) - {}^{(n)}k_{2i}s({}^{(n)}\mu_i), \tag{28}$$

$${}^{(n)}Z_i = {}^{(n)}k_{1i}s({}^{(n)}\mu_i) - {}^{(n)}k_{2i}c({}^{(n)}\mu_i), \tag{29}$$

where

$${}^{(n)}k_{1i} = a + bc({}^{(n)}\vartheta_{2i}), \tag{30}$$

$${}^{(n)}k_{2i} = bs({}^{(n)}\vartheta_{2i}). \tag{31}$$

From which:

$$s{}^{(n)}\mu_i = \frac{{}^{(n)}k_{1i}{}^{(n)}Z_i - {}^{(n)}k_{2i}{}^{(n)}Y_i}{{}^{(n)}k_{1i}{}^2 + {}^{(n)}k_{2i}{}^2}, \tag{32}$$

$$c{}^{(n)}\mu_i = \frac{{}^{(n)}k_{2i}{}^{(n)}Z_i + {}^{(n)}k_{1i}{}^{(n)}Y_i}{{}^{(n)}k_{1i}{}^2 + {}^{(n)}k_{2i}{}^2}, \tag{33}$$

and finally

$${}^{(n)}\mu_i = {}^{(n)}\vartheta_{1i} = \text{atan2}[s{}^{(n)}\mu_i, c{}^{(n)}\mu_i]. \tag{34}$$

Then, the inverse kinematics has four solutions for each ϑ_{1i} ($i = 1, 2, 3$). Indeed, given the Euler's angles, for each leg i two values of λ_i can be obtained. For each λ_i Eq. (27) provides two values for ϑ_{2i}. Equation (34), instead, provides an unique value of ϑ_{1i} for a given ϑ_{2i}. Therefore, a total of 4^3 combinations of the input variables ϑ_{1i} ($i = 1, 2, 3$) may be possible.

5. Direct Kinematics

In direct kinematics, the actuated rotations ϑ_{1i} ($i = 1, 2, 3$) are given, whilst the Euler's angles ϕ, γ, ψ of the moving platform must be calculated. Once again, Eqs. (16) and (19) are used to obtain the solution. In much the same way as with the procedure of the inverse position kinematics ϑ_{3i}, ϑ_{2i} are calculated by manipulating Eq. (21). Separating the unknowns from known terms they can be written as

$$V_i = P_{yi} - ac(\mu_i) = bc(\chi_i) + dc(\lambda_i), \tag{35}$$

$$W_i = P_{zi} - as(\mu_i) = bs(\chi_i) + ds(\lambda_i). \tag{36}$$

First, we square both Eqs. (35) and (36) and add them; then we use the trigonometric relation

$$s(\chi_i)s(\lambda_i) = c(\lambda_i - \chi_i) - c(\lambda_i)c(\chi_i) \tag{37}$$

https://doi.org/10.1017/S0263574709990683 Published online by Cambridge University Press

to obtain

$$^{(n)}\vartheta_{3i} = \text{acos}\left[\frac{(V_i)^2 + (Z_i)^2 - b^2 - d^2}{2bd}\right]. \tag{38}$$

Equation (38) provides two solutions for $^{(n)}\vartheta_{3i}$ $(n = 1, 2)$. Having $^{(n)}\vartheta_{3i}$ Eqs. (35) and (36) can be solved for $^{(n)}\vartheta_{2i}$. By expanding the terms and collecting the known values Eqs. (35) and (36) lead to

$$^{(n)}V_i = {}^{(n)}y_{1i}c(^{(n)}\vartheta_{2i}) - {}^{(n)}y_{2i}s(^{(n)}\vartheta_{2i}), \tag{39}$$

$$^{(n)}W_i = {}^{(n)}y_{1i}s(^{(n)}\vartheta_{2i}) + {}^{(n)}y_{2i}c(^{(n)}\vartheta_{2i}), \tag{40}$$

where

$$^{(n)}y_{1i} = bc(^{(n)}\vartheta_{1i}) + dc(^{(n)}\vartheta_{1i} + {}^{(n)}\vartheta_{3i}), \tag{41}$$

$$^{(n)}y_{2i} = bs(^{(n)}\vartheta_{1i}) + ds(^{(n)}\vartheta_{1i} + {}^{(n)}\vartheta_{3i}), \tag{42}$$

from which

$$s(^{(n)}\vartheta_{2i}) = \frac{{}^{(n)}y_{1i}{}^{(n)}W_i - {}^{(n)}y_{2i}{}^{(n)}V_i}{{}^{(n)}y_{1i}{}^2 + {}^{(n)}y_{2i}{}^2}, \tag{43}$$

$$c(^{(n)}\vartheta_{2i}) = \frac{{}^{(n)}y_{2i}{}^{(n)}W_i + {}^{(n)}y_{1i}{}^{(n)}V_i}{{}^{(n)}y_{1i}{}^2 + {}^{(n)}y_{2i}{}^2}, \tag{44}$$

and finally

$$^{(n)}\vartheta_{2i} = \text{atan2}\big[s(^{(n)}\vartheta_{2i}), c(^{(n)}\vartheta_{2i})\big]. \tag{45}$$

To obtain ϕ, γ, ψ explicitly a Euler's convention is to be chosen for ${}^0\mathbf{R}_G$. Consider the rotation of the moving platform as a rotation ϕ about the Z_G axis, followed by a rotation γ about the rotated X_G axis, namely $X_G^{'}$, followed by a rotation ψ about the rotated Y_G axis, namely $Y_G^{''}$. Thus, ${}^0\mathbf{R}_G$ becomes

$$\begin{aligned} {}^0\mathbf{R}_G &= \mathbf{R}_{Z_G}(\phi)\mathbf{R}_{X_G^{'}}(\gamma)\mathbf{R}_{Y_G^{''}} \\ &= \begin{bmatrix} -s\phi s\gamma s\psi + c\phi c\psi & -s\phi c\gamma & s\phi s\gamma c\psi + c\phi s\psi \\ c\phi s\gamma s\psi + s\phi c\psi & c\phi c\gamma & -c\phi s\gamma c\psi + s\phi s\psi \\ -c\gamma s\psi & s\gamma & c\gamma c\psi \end{bmatrix}. \end{aligned} \tag{46}$$

At this point, Eq. (19) can be written for each leg with only the Euler's angles as unknown:

$$c\lambda_1(-c\phi s\gamma c\psi + s\phi s\psi) + s\lambda_1(c\gamma c\psi) = 0, \tag{47}$$

$$c\lambda_2(-s\phi s\gamma s\psi + c\phi c\psi) + s\lambda_2(c\gamma s\psi) = 0, \tag{48}$$

$$c\lambda_3(s\phi c\gamma) + s\lambda_3(c\phi c\gamma) = 0. \tag{49}$$

From Eq. (49)

$$\phi = \text{atan}\left(\frac{-s\lambda_3}{c\lambda_3}\right). \tag{50}$$

The solutions of (50) are two-spaced each to the other by π. Equations (47), (48) can be expressed as

$$J_1 s\gamma + K_1 c\gamma + L_1 = 0, \tag{51}$$

$$J_2 s\gamma + K_2 c\gamma + L_2 = 0, \tag{52}$$

where

$$\begin{array}{lll} J_1 = -A_1 c\phi c\psi & K_1 = B_1 c\psi & L_1 = A_1 s\phi s\psi, \\ J_2 = -A_2 s\phi s\psi & K_2 = B_2 s\psi & L_2 = A_2 c\phi c\psi \end{array} \tag{53}$$

with

$$A_i = c\lambda_i, \qquad B_i = s\lambda_i, \qquad (i = 1, 2, 3).$$

Equations (51) and (52) can be solved for sγ and cγ:

$$\begin{aligned} s\gamma &= -L_1 K_2 + K_1 L_2 - K_1 J_2 + J_1 K_2, \\ c\gamma &= L_1 J_2 - J_1 L_2 - J_1 K_2 - K_1 J_2. \end{aligned} \tag{54}$$

Substituting Eq. (54) into the trigonometric identity $s^2\gamma + c^2\gamma = 1$ provides a nonlinear equation with only ψ as an unknown:

$$(A^{'} + B^{'} - C^{'})s^4\psi + (C^{'} - 2A^{'})s^2\psi + A^{'} = 0, \tag{55}$$

where

$$\begin{aligned} A^{'} &= \left(A_2^2 B_1^2 c^2\phi + A_1^2 A_2^2 c^4\phi\right), \\ B^{'} &= \left(A_1^2 B_2^2 s^2\phi + A_1^2 A_2^2 s^4\phi\right), \\ C^{'} &= -\left(A_2^2 B_1^2 s^2\phi + A_1^2 B_2^2 c^2\phi + 2A_1^2 A_2^2 s^2\phi c^2\phi\right). \end{aligned} \tag{56}$$

Equation (55) provides four solutions for sψ and thus eight possible solutions for ψ at most. By simple back-substitution in Eq. (54), γ is obtained univocally by using the two-argument arctangent function. As a matter of fact ϕ can assume two values from Eq. (50), ψ can assume eight values from Eq. (55), whose coefficients have no dependence on which ϕ is used and γ can assume sixteen values from Eqs. (54) whose coefficients depend on both ϕ and ψ. Thus, considering all the possible combinations there are theoretically 128 sets of Euler's angles and 64 possible poses of the moving platform for given actuated rotations. However, an inpection on these solutions show that only 32 solutions are distinct. This result was obtained independently in [15]. Equations (50) and (54) are obtained with $\gamma, \phi \neq \pi/2$, $c\lambda_3 \neq 0$ and $J_1 K_2 \neq K_1 J_2$.

Cases when $\gamma = \pm\pi/2$, $\phi = \pm\pi/2$ and $J_1 K_2 = K_1 J_2$ are addressed in detail as follows.

Case $\gamma = \pm\pi/2$:

In this case Eq. (49) is satisfied for any value of λ_3 that means for any value of $\sum_{i=1}^{3}\vartheta_{i3}$.

Equation (48) can be satisfied if

$$\lambda_2 = \sum_{i=1}^{3}\vartheta_{i2} = \pm\pi/2 \text{ or } \phi + \psi = \pm\pi/2.$$

https://doi.org/10.1017/S0263574709990683 Published online by Cambridge University Press

Table I. Input Parameters (in radians).

λ_1	λ_2	λ_3
3.2316	1.9906	3.8226

Identically Eq. (47) can be satisfied if

$$\lambda_1 = \sum_{i=1}^{3} \vartheta_{i1} = \pm\pi/2 \text{ or } \phi + \psi = \pm\pi/2.$$

Case $\phi = \pm\pi/2$:
In this case Eq. (49) is satisfied if and only if:

$$\sum_{i=1}^{3} \vartheta_{i3} = \pm\pi/2$$

Equations (47) and (48) form a system of two nonlinear equation with two unknowns:

$$c\lambda_1 s\psi + s\lambda_1(c\gamma c\psi) = 0, \tag{57}$$

$$-c\lambda_2 s\gamma s\psi + s\lambda_2(c\gamma s\psi) = 0. \tag{58}$$

Equation (58) has solutions $\psi = 0$ or $\gamma = \lambda_2$.
If $\psi = 0$ then Eq. (57) is satisfied when:

$$\sum_{i=1}^{3} \vartheta_{i1} = 0 \text{ or } \gamma = \pm\pi/2.$$

If $\gamma = \lambda_2$ then Eq. (57) is satisfied when:

$$\psi = 2\text{atan}\left(\frac{c\lambda_1 \pm \sqrt{(c\lambda_1)^2 - (s\lambda_1 c\gamma)^2}}{s\lambda_1 c\gamma}\right). \tag{59}$$

Case $J_1K_2 = K_1J_2$:
This equation is expressed as

$$s\psi c\psi(c\lambda_1 s\lambda_2 c\phi - s\lambda_1 c\lambda_2 s\phi) = 0. \tag{60}$$

Equation (60) is satisfied when:

$$\psi = 0 \text{ or } \phi = 2\text{atan}\left(\frac{-c\lambda_2 s\lambda_1 \pm \sqrt{(c\lambda_2 s\lambda_1)^2 - (c\lambda_1 s\lambda_2)^2}}{c\lambda_1 s\lambda_2}\right).$$

To illustrate the plurality of the solutions of the direct kinematics position analysis, a numerical example is now presented. Solutions are obtained by solving Eq. (50) for ϕ, Eq. (55) for ψ and by using Eqs. (54) in the two-argument arctangent function to obtain γ. Finally, ${}^0\mathbf{R}_G$ is obtained according to the definition given in Eq. (46).

In Table I the input parameters are shown, Table II show the Euler's angles from calculation. In Table II, ψ_l $(l = 1, \ldots, 8)$ are obtained from Eq. (55), whatever ϕ_k $(k = 1,2)$ is used. From Eqs. (54), γ takes values γ_m $(m = 1, \ldots, 8)$ for ϕ_1 and ψ_l $(l = 1, \ldots, 8)$ and values γ_m $(m = 9, \ldots, 16)$ for ϕ_2 and ψ_l $(l = 1, \ldots, 8)$. Table III shows four solutions of the 32 distinct rotation matrices*.

* The complete numerical example can be provided by the authors upon request.

Table II. Euler's angles (in radians).

ϕ_k	ψ_l	γ_m
	0.8898	−0.8454
	−0.8898	1.2741
	0.3242	−0.1073
−0.6810	−0.3242	2.9108
	−0.8898	1.2741
	0.8898	−0.8454
	−0.3242	2.9108
	0.3242	−40.1073
	0.8898	−1.2741
	−0.8898	0.8454
	0.3242	−2.9108
2.4606	−0.3242	0.1073
	−0.8898	0.8454
	0.8898	−1.2741
	−0.3242	0.1073
	0.3242	−2.9108

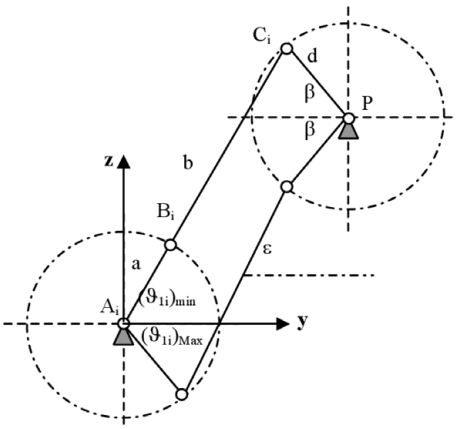


Fig. 3. Geometry of the ith leg as a four-bar planar linkage.

6. Numerical Example of Calculation of the Workspace

Calculation of the workspace in the Euler's space was carried out. It consisted of solving the direct position analysis by imposing the variation of ϑ_{1i}. The procedure proposed consisted of three steps:

- (i) Define the range limits ϑ_{1imin} and ϑ_{1iMax} for the actuated angles;
- (ii) For each value ϑ_{1i} $(i = 1, 2, 3)$ given, evaluate the passive angles ϑ_{3i}, ϑ_{2i};
- (iii) Solve the nonlinear Eqs. (47), (48), and (49).

(i) The actuated pairs ϑ_{1i} must respect the limits imposed by the leg geometry varying between ϑ_{1imin} and ϑ_{1iMax}. Indeed, a single leg can be analyzed just as a planar four-bar linkage, with A_i and P as fixed revolute pairs and d as virtual link (Fig. 3). The lower limit position of the linkage is set when $\vartheta_{2i} = 0$ (first and second link aligned). The upper limit position is obtained by geometry, considering a symmetric rotation β of the virtual link around a direction perpendicular to the plane of motion and passing through P, which coincides with each of the $\{G\}$ axes at the nominal pose.

By a procedure similar to those exploited for both the direct and inverse position analyses the planar linkage geometry at

https://doi.org/10.1017/S0263574709990683 Published online by Cambridge University Press

Table III. Examples of rotation matrices (poses).

$$^0\mathbf{R}_G = \begin{bmatrix} 0.1231 & 0.4176 & 0.9002 \\ -0.8480 & 0.5154 & -0.1231 \\ -0.5154 & -0.7483 & 0.4176 \end{bmatrix} \quad ^0\mathbf{R}_G = \begin{bmatrix} 0.9569 & 0.1841 & 0.2247 \\ 0.1810 & 0.2272 & -0.9569 \\ -0.2272 & 0.9563 & 0.1841 \end{bmatrix}$$

$$^0\mathbf{R}_G = \begin{bmatrix} 0.4367 & 0.6259 & 0.6461 \\ -0.4610 & 0.7725 & -0.4367 \\ -0.7725 & -0.1071 & 0.6259 \end{bmatrix} \quad ^0\mathbf{R}_G = \begin{bmatrix} 0.6010 & -0.6129 & 0.5130 \\ -0.2582 & -0.7564 & -0.6010 \\ 0.7564 & 0.2288 & -0.6129 \end{bmatrix}$$

the lower limit position leads to:

$$P_{yi} = (a+b)c\vartheta_{1imin} + dc\beta \tag{61}$$

$$P_{zi} = (a+b)s\vartheta_{1imin} - ds\beta \tag{62}$$

First we square both Eqs. (61) and (62) and add them; then we use a trigonometric relation to obtain:

$$\tilde{\beta} = \vartheta_{1imin} + \beta = \text{acos}\left(\frac{{P_{yi}}^2 + {P_{zi}}^2 - [(a+b)^2 + d^2]}{2(a+b)d}\right) \tag{63}$$

Therefore Eqs. (61), (62) can be rewritten as:

$$P_{yi} = (a+b)c\vartheta_{1imin} + dc(\tilde{\beta} - \vartheta_{1imin}) \tag{64}$$

$$P_{zi} = (a+b)s\vartheta_{1imin} - ds(\tilde{\beta} - \vartheta_{1imin}) \tag{65}$$

By expanding the terms and collecting the known values Eqs. (64), (65) lead to:

$$P_{yi} = R_1 c\vartheta_{1imin} + T_1 s\vartheta_{1imin} \tag{66}$$

$$P_{zi} = R_1 s\vartheta_{1imin} - T_1 c\vartheta_{1imin} \tag{67}$$

where

$$R_1 = (a+b) + dc\tilde{\beta}$$

$$T_1 = ds\tilde{\beta}$$

Equations (66), (67) can easily be solved for ϑ_{1imin}:

$$\vartheta_{1imin} = \text{asin}\left(\frac{P_{zi}R_1 + P_{yi}T_1}{R_1^2 + T_1^2}\right) \tag{68}$$

Calculation to obtain ϑ_{1iMax} starts from the analysis of the linkage at the upper position:

$$P_{yi} - dc\beta = ac\vartheta_{1iMax} + bc\epsilon \tag{69}$$

$$P_{zi} - ds\beta = -as\vartheta_{1iMax} + bs\epsilon \tag{70}$$

where

$$\beta = \tilde{\beta} - \vartheta_{1imin}$$

β is known from previous calculation, ϵ is the angle that B_iC_i forms with a reference direction (Fig. 3). We square Eqs. (69), (70), add them and use a trigonometric relation to obtain:

$$\epsilon + \vartheta_{1iMax} = \tilde{\epsilon} = \text{acos}\left(\frac{P_{y1}^2 + P_{z2}^2 - a^2 - b^2}{2ab}\right) \tag{71}$$

Therefore Eqs. (69), (70) can be rewritten as:

$$P_{Yi} = ac\vartheta_{1iMax} + bc(\tilde{\epsilon} - \vartheta_{1iMax}) \tag{72}$$

$$P_{zi} = as\vartheta_{1iMax} - bs(\tilde{\epsilon} - \vartheta_{1iMax}) \tag{73}$$

By expanding the terms and collecting the known values Eqs. (72), (73) lead to:

$$P_{Yi} = R_2 c\vartheta_{1iMax} + T_2 s\vartheta_{1iMax} \tag{74}$$

$$P_{zi} = -R_2 s\vartheta_{1iMax} + T_2 c\vartheta_{1iMax} \tag{75}$$

where

$$R_2 = a + b + c\tilde{\epsilon}$$

$$T_2 = bs\tilde{\epsilon}$$

Equations (74), (75) can easily be solved for ϑ_{1iMax}:

$$\vartheta_{1iMax} = \text{asin}\left(\frac{P_{Yi}T_2 - P_{zi}R_2}{R_2^2 + T_2^2}\right) \tag{76}$$

(ii) ϑ_{1i}'s $i = 1, 2, 3$ vary between ϑ_{1imin}, ϑ_{1iMax} to cover a full combination of given data. For each combination, step k of the calculation, the passive angles ϑ_{3i}, ϑ_{2i} were obtained by Eqs. (38), (45), respectively. Out of the two possible postures of each leg, the elbow-up posture was selected in all cases.

(iii) The nonlinear Eqs. (47), (48), (49) were solved by the Gauss-Newton iterative method implemented in the *fsolve* command of *Matlab* code. The method allows us to select the appropriate solution out of the possible 32 distinct solutions obtained in Section 5 by the analytical procedure. Indeed, the unique pose adopted by the manipulator at step k will be the closest to the previous one adopted at step k-1 starting from the nominal pose of the moving platform. The method required the guess values for the Euler's angles. They were selected to be zero at the first step of the calculation and to be the results of the k-1 step at the k step of the calculation. This procedure fails whenever the manipulator passes through a singularity causing a branch-jump. As a numerical example, a

https://doi.org/10.1017/S0263574709990683 Published online by Cambridge University Press

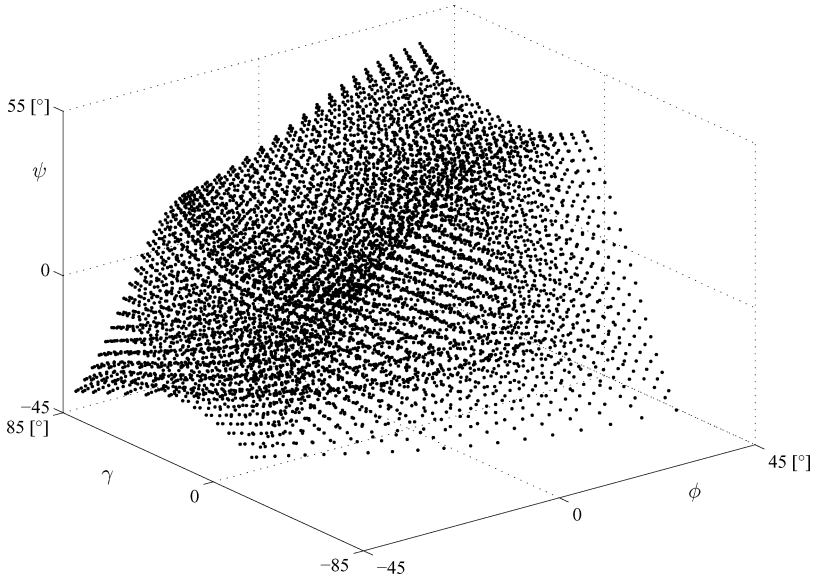


Fig. 4. Euler's angles workspace.

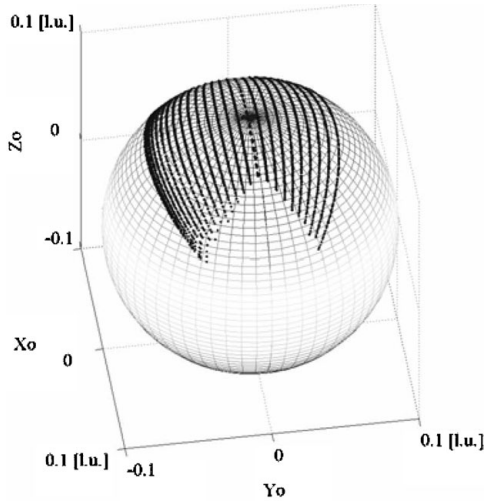


Fig. 5. Cartesian workspace of a reference point on the moving platform.

workspace was calculated with $a = d = 0.5$ and $b = 1$ (length unit [l.u.]). Figure 4 shows the Euler's workspace. From Fig. 4, it can be seen that ϕ is in the range from about -45° to about 35°; similarly, ψ is in the range from about -45° to about 50° whilst γ is in the range of $\pm 80^\circ$. The results obtained are used to calculate the locus of points reached by a reference point on the moving platform located by ${}^G\mathbf{v_1} = [0\ 0\ 0.1]^T$ [l.u.]. These points lie on the theoretical workspace which is a complete sphere with radius 0.1 l.u. and centered in P. The Cartesian workspace of that reference point is shown in Fig. 5.

7. Differential Kinematics

In order to obtain the relationships between the actuated rotation rates $\dot{\boldsymbol{\theta}}_1 = [\dot{\vartheta}_{11}\ \dot{\vartheta}_{12}\ \dot{\vartheta}_{13}]^T$ and the angular velocity of the moving platform $\boldsymbol{\omega}$, expressed as $\dot{\boldsymbol{\theta}}_1 = \mathbf{J}\boldsymbol{\omega}$, where $\mathbf{J}$ denotes the jacobian matrix, Eq. (11) is differentiated with respect to time:

$$\frac{\mathrm{d}}{\mathrm{d}t}\hat{\mathbf{w}}_i \cdot \hat{\mathbf{v}}_i + \hat{\mathbf{w}}_i \cdot \frac{\mathrm{d}}{\mathrm{d}t}\hat{\mathbf{v}}_i = (\dot{\vartheta}_{1i} + \dot{\vartheta}_{2i} + \dot{\vartheta}_{3i})\mathbf{x}_{1i} \times \hat{\mathbf{w}}_i \cdot \hat{\mathbf{v}}_i + \boldsymbol{\omega} \times \hat{\mathbf{v}}_i \cdot \hat{\mathbf{w}}_i = 0. \tag{77}$$

$\dot{\vartheta}_{2i}, \dot{\vartheta}_{3i}$ may be expressed in terms of $\dot{\vartheta}_{1i}$ dot-multiplying Eq. (4) by $\mathbf{l}_i$ and $\mathbf{d}_i$, respectively:

$$\dot{\vartheta}_{1i}\mathbf{x}_{1i} \times \mathbf{s}_i \cdot \mathbf{l}_i + \dot{\vartheta}_{3i}\mathbf{x}_{1i} \times \mathbf{d}_i \cdot \mathbf{l}_i = 0, \tag{78}$$

from which, by simple manipulations:

$$\dot{\vartheta}_{3i} = -\dot{\vartheta}_{1i}\frac{\mathbf{x}_{1i} \cdot \mathbf{s}_i \times \mathbf{l}_i}{\mathbf{x}_{1i} \cdot \mathbf{d}_i \times \mathbf{l}_i} = -\dot{\vartheta}_{1i}\frac{\mathbf{x}_{1i} \cdot \mathbf{s}_i \times \mathbf{l}_i}{\mathbf{x}_{1i} \cdot \mathbf{d}_i \times \mathbf{b}_i} \tag{79}$$

Similarly,

$$\dot{\vartheta}_{1i}\mathbf{x}_{1i} \times \mathbf{s}_i \cdot \mathbf{d}_i + \dot{\vartheta}_{2i}\mathbf{x}_{1i} \times \mathbf{l}_i \cdot \mathbf{d}_i = 0 \tag{80}$$

from which, by simple manipulations:

$$\dot{\vartheta}_{2i} = \dot{\vartheta}_{1i}\frac{\mathbf{x}_{1i} \cdot \mathbf{s}_i \times \mathbf{d}_i}{\mathbf{x}_{1i} \cdot \mathbf{d}_i \times \mathbf{b}_i}. \tag{81}$$

Introducing Eqs. (79) and (81) into Eq. (77) and exploiting the distributive law of the cross product leads to:

$$-\dot{\vartheta}_{1i}\left(\frac{\mathbf{x}_{1i} \cdot \mathbf{a}_i \times \mathbf{b}_i}{\mathbf{x}_{1i} \cdot \mathbf{d}_i \times \mathbf{b}_i}\right)\mathbf{x}_{1i} \times \hat{\mathbf{w}}_i \cdot \hat{\mathbf{v}}_i + \boldsymbol{\omega} \times \hat{\mathbf{v}}_i \cdot \hat{\mathbf{w}}_i = 0 \tag{82}$$

from which

$$\dot{\vartheta}_{1i} = \left(\frac{\hat{\mathbf{v}}_i \times \hat{\mathbf{w}}_i}{\left(\frac{\mathbf{x}_{1i} \cdot \mathbf{a}_i \times \mathbf{b}_i}{\mathbf{x}_{1i} \cdot \mathbf{d}_i \times \mathbf{b}_i}\right)\mathbf{x}_{1i} \times \hat{\mathbf{w}}_i \cdot \hat{\mathbf{v}}_i}\right) \cdot \boldsymbol{\omega}. \tag{83}$$

https://doi.org/10.1017/S0263574709990683 Published online by Cambridge University Press

Thus, the ith row of the Jacobian matrix is given as

$$\mathbf{J}_i = \begin{pmatrix} \hat{\mathbf{w}}_i \times \hat{\mathbf{v}}_i \\ \hline \left(\dfrac{\mathbf{x}_{1i} \cdot \mathbf{a}_i \times \mathbf{b}_i}{\mathbf{x}_{1i} \cdot \mathbf{b}_i \times \mathbf{d}_i}\right) \mathbf{x}_{1i} \times \hat{\mathbf{w}}_i \cdot \hat{\mathbf{v}}_i \end{pmatrix}. \tag{84}$$

8. Isotropy and Singularities

From Gosselin *et al.*,[5] in order to inspect for the existence of singularities, the relationship between $\dot{\boldsymbol{\theta}}_1$ and $\boldsymbol{\omega}$ can be expressed as

$$\mathbf{A}\boldsymbol{\omega} + \mathbf{B}\dot{\boldsymbol{\theta}}_1 = 0, \tag{85}$$

where

$$\mathbf{J} = -\mathbf{B}^{-1}\mathbf{A}, \tag{86}$$

$$\mathbf{A} = \begin{bmatrix} \hat{\mathbf{w}}_1 \times \hat{\mathbf{v}}_1 \\ \hat{\mathbf{w}}_2 \times \hat{\mathbf{v}}_2 \\ \hat{\mathbf{w}}_3 \times \hat{\mathbf{v}}_3 \end{bmatrix}, \tag{87}$$

$$\mathbf{B} = \begin{bmatrix} \left(\dfrac{\mathbf{x}_{11} \cdot \mathbf{a}_1 \times \mathbf{b}_1}{\mathbf{x}_{11} \cdot \mathbf{b}_1 \times \mathbf{d}_1}\right) \mathbf{x}_{11} \times \hat{\mathbf{w}}_1 \cdot \hat{\mathbf{v}}_1 & 0 & 0 \\ 0 & \left(\dfrac{\mathbf{x}_{12} \cdot \mathbf{a}_2 \times \mathbf{b}_2}{\mathbf{x}_{12} \cdot \mathbf{b}_2 \times \mathbf{d}_2}\right) \mathbf{x}_{12} \times \hat{\mathbf{w}}_2 \cdot \hat{\mathbf{v}}_2 & 0 \\ 0 & 0 & \left(\dfrac{\mathbf{x}_{13} \cdot \mathbf{a}_3 \times \mathbf{b}_3}{\mathbf{x}_{13} \cdot \mathbf{b}_3 \times \mathbf{d}_3}\right) \mathbf{x}_{13} \times \hat{\mathbf{w}}_3 \cdot \hat{\mathbf{v}}_3 \end{bmatrix}. \tag{87}$$

It is well known that for parallel manipulators two kinds of singularities may occur[1]. In direct kinematic singularity (parallel singularity) $det(\mathbf{J}) = 0$ ($det(\mathbf{A}) = 0$) the manipulator gains an unwanted degree of freedom. This condition, for 3-RRUR manipulator, may occur only if the three vectors $\hat{\mathbf{n}}_i = \hat{\mathbf{w}}_i \times \hat{\mathbf{v}}_i$ $(i = 1, 2, 3)$ are coplanar. The condition is analyzed as follows.

By definition:

$$\begin{aligned} \hat{\mathbf{v}}_1 &= \hat{\mathbf{v}}_3 \times \hat{\mathbf{v}}_2, \\ \hat{\mathbf{v}}_2 &= \hat{\mathbf{v}}_1 \times \hat{\mathbf{v}}_3, \\ \hat{\mathbf{v}}_3 &= \hat{\mathbf{v}}_2 \times \hat{\mathbf{v}}_1. \end{aligned} \tag{88}$$

Introducing Eq. (88) into the definition of $\hat{\mathbf{n}}_i$s:

$$\begin{aligned} \hat{\mathbf{n}}_1 &= \hat{\mathbf{w}}_1 \times \hat{\mathbf{v}}_1 = \hat{\mathbf{w}}_1 \cdot \hat{\mathbf{v}}_2 \hat{\mathbf{v}}_3 - \hat{\mathbf{w}}_1 \cdot \hat{\mathbf{v}}_3 \hat{\mathbf{v}}_2, \\ \hat{\mathbf{n}}_2 &= \hat{\mathbf{w}}_2 \times \hat{\mathbf{v}}_2 = \hat{\mathbf{w}}_2 \cdot \hat{\mathbf{v}}_3 \hat{\mathbf{v}}_1 - \hat{\mathbf{w}}_2 \cdot \hat{\mathbf{v}}_1 \hat{\mathbf{v}}_3, \\ \hat{\mathbf{n}}_3 &= \hat{\mathbf{w}}_3 \times \hat{\mathbf{v}}_3 = \hat{\mathbf{w}}_3 \cdot \hat{\mathbf{v}}_3 \hat{\mathbf{v}}_3 - \hat{\mathbf{w}}_3 \cdot \hat{\mathbf{v}}_2 \hat{\mathbf{v}}_1. \end{aligned} \tag{89}$$

Equations (89) state that $\hat{\mathbf{n}}_1$ belongs to a plane formed by $\hat{\mathbf{v}}_2$ and $\hat{\mathbf{v}}_3$, $\hat{\mathbf{n}}_2$ belongs to a plane formed by $\hat{\mathbf{v}}_1$ and $\hat{\mathbf{v}}_3$ and $\hat{\mathbf{n}}_3$ belongs to a plane formed by $\hat{\mathbf{v}}_1$ and $\hat{\mathbf{v}}_2$. The planes formed by $\hat{\mathbf{v}}_1\hat{\mathbf{v}}_2$, $\hat{\mathbf{v}}_2\hat{\mathbf{v}}_3$, $\hat{\mathbf{v}}_1\hat{\mathbf{v}}_3$ coincide with the faces of the tetrahedron which are perpendicular each to the others. Therefore, in the general case $\hat{\mathbf{n}}_1$, $\hat{\mathbf{n}}_2$, $\hat{\mathbf{n}}_3$ cannot be coplanar. However, three special conditions leading to singularity are to be addressed separately:

(1) $\hat{\mathbf{n}}_1$ and $\hat{\mathbf{n}}_3$ are parallel to $\hat{\mathbf{v}}_2$ whereas $\hat{\mathbf{n}}_2$ can be parallel to $\hat{\mathbf{v}}_1$ or to $\hat{\mathbf{v}}_3$. From the first and the third of the Eqs. (89):

$$\begin{aligned} \hat{\mathbf{n}}_1 \cdot \hat{\mathbf{v}}_3 &= \hat{\mathbf{w}}_1 \cdot \hat{\mathbf{v}}_2 = 0, \\ \hat{\mathbf{n}}_3 \cdot \hat{\mathbf{v}}_1 &= \hat{\mathbf{w}}_3 \cdot \hat{\mathbf{v}}_2 = 0. \end{aligned}$$

Moreover, because of Eq. (11), $\hat{\mathbf{w}}_2 \cdot \hat{\mathbf{v}}_2 = 0$. Therefore $\hat{\mathbf{w}}_i$ are to be coplanar.

(2) $\hat{\mathbf{n}}_1$ and $\hat{\mathbf{n}}_2$ are parallel to $\hat{\mathbf{v}}_3$ whereas $\hat{\mathbf{n}}_3$ can be parallel to $\hat{\mathbf{v}}_1$ or to $\hat{\mathbf{v}}_2$. From the first and the second of the Eqs. (89):

$$\begin{aligned} \hat{\mathbf{n}}_1 \cdot \hat{\mathbf{v}}_2 &= \hat{\mathbf{w}}_1 \cdot \hat{\mathbf{v}}_3 = 0, \\ \hat{\mathbf{n}}_2 \cdot \hat{\mathbf{v}}_1 &= \hat{\mathbf{w}}_2 \cdot \hat{\mathbf{v}}_3 = 0, \end{aligned}$$

and considering that $\hat{\mathbf{w}}_3 \cdot \hat{\mathbf{v}}_3 = 0$ from Eq. (11) then $\hat{\mathbf{w}}_i$ are to be coplanar.

(3) $\hat{\mathbf{n}}_1$ and $\hat{\mathbf{n}}_3$ are parallel to $\hat{\mathbf{v}}_2$ whereas $\hat{\mathbf{n}}_2$ can be parallel to $\hat{\mathbf{v}}_1$ or to $\hat{\mathbf{v}}_3$. From the second and the third of the Eqs. (89):

$$\begin{aligned} \hat{\mathbf{n}}_1 \cdot \hat{\mathbf{v}}_3 &= \hat{\mathbf{w}}_2 \cdot \hat{\mathbf{v}}_1 = 0, \\ \hat{\mathbf{n}}_3 \cdot \hat{\mathbf{v}}_1 &= \hat{\mathbf{w}}_3 \cdot \hat{\mathbf{v}}_1 = 0, \end{aligned}$$

and by means of $\hat{\mathbf{w}}_1 \cdot \hat{\mathbf{v}}_1 = 0$ from Eq. (11) it is obtained that $\hat{\mathbf{w}}_i$ are to be coplanar.

Therefore, the manipulator has direct kinematic singularities whenever $\hat{\mathbf{w}}_i$, $(i = 1, 2, 3)$ are coplanar.

In the inverse kinematic singularity (serial singularity) $det(\mathbf{J}) = \infty$ ($det(\mathbf{B}) = 0$), the moving platform may not move even if some actuated rotations are given. This condition, for 3-RRUR manipulator, may arise if $(\frac{\mathbf{x}_{1i} \cdot \mathbf{a}_i \times \mathbf{b}_i}{\mathbf{x}_{1i} \cdot \mathbf{b}_i \times \mathbf{c}_i})\mathbf{x}_{1i}$, $\hat{\mathbf{w}}_i$ and $\hat{\mathbf{v}}_i$ are coplanar and if at least one of $\mathbf{a}_i \times \mathbf{b}_i = 0$. Since $(\frac{\mathbf{x}_{1i} \cdot \mathbf{a}_i \times \mathbf{b}_i}{\mathbf{x}_{1i} \cdot \mathbf{b}_i \times \mathbf{d}_i})\mathbf{x}_{1i}$ and $\hat{\mathbf{w}}_i$ are always perpendicular the first condition is matched only when $\hat{\mathbf{v}}_i$ is parallel to $\mathbf{x}_{1i}$. Theoretically, inverse singularities may occur when the first and last R pair axes of a leg are aligned and when at least one of the legs is fully folded or stretched.

To qualitatively describe the motion of a moving platform the performance index $\zeta(\mathbf{J})$ is introduced[1]. The index $\zeta(\mathbf{J})$ is the inverse of the condition number $\kappa(\mathbf{J})$ defined as

$$\kappa(\mathbf{J}) = \|\mathbf{J}\| \|\mathbf{J}^{-1}\|, \tag{90}$$

where

$$\|\mathbf{J}\| = \sqrt{trace(\mathbf{J}^T \mathbf{W} \mathbf{J})}. \tag{91}$$

$\|\mathbf{J}\|$ s the Frobenius norm of $\mathbf{J}$. $\mathbf{W}$ is a weighting matrix equal to $\mathbf{I}/3$. A value of zero for $\zeta(\mathbf{J})$ denotes a singular pose, whereas a value of 1 denotes an isotropic configuration, i.e., a perfectly conditioned $\mathbf{J}$ matrix. Calculation of $\zeta(\mathbf{J})$ is

https://doi.org/10.1017/S0263574709990683 Published online by Cambridge University Press

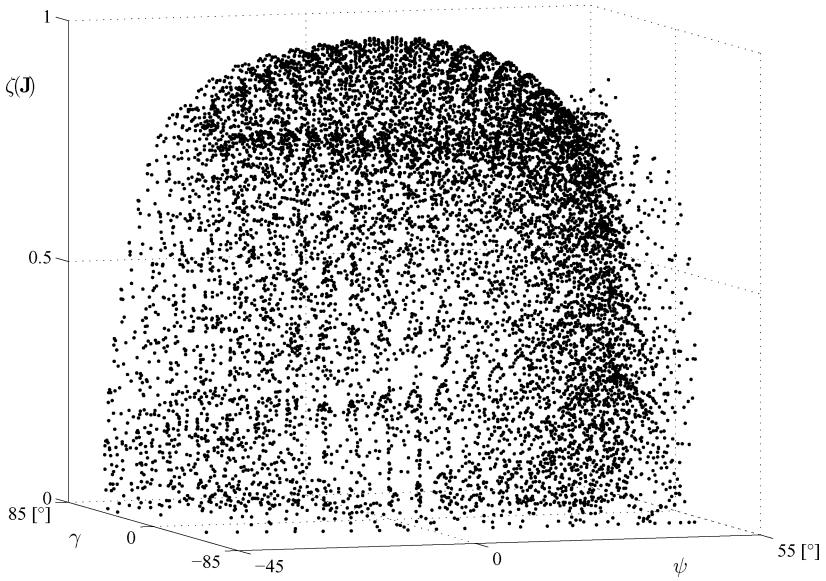


Fig. 6. $\zeta(\mathbf{J})$ vs. ψ, γ.

appended to the procedure presented in Section 6 to obtain the workspace. $\zeta(\mathbf{J})$ at step k is calculated through calculation of **A** and **B** and by Eqs. (86), (90), (91) against the Euler's angles.

Figures 6, 7, and 8 give the values of $\zeta(\mathbf{J})$. The manipulator has $\zeta(\mathbf{J}) = 1$ at the nominal pose where $\phi = \gamma = \psi = 0$. About 20% of points reached in the workspace give $\zeta(\mathbf{J}) < 0.25$, indicating a manipulator behavior far from isotropy. One percent of these points are lower than 0.01 showing a badly conditioned **J** matrix. About 35% of the points have $\zeta(\mathbf{J}) > 0.75$, indicating a manipulator behavior close to isotropy.

9. Mechanical Interference

In this section the condition matched in the case of mechanical interference is addressed. Mechanical interference can occur when the last link of a leg intersect the last link of an other leg. In this section the last link of each leg is an arc centered in P and with radius $r = h = d$. By naming H_i the mid-line point on the arc of leg i, the interference condition between leg i and leg j is matched whenever

$$|\mathbf{H}_j\mathbf{H}_i| = 0. \tag{92}$$

According to Fig. 9 Eq. (92) can be written as

$$|\mathbf{H}_j\mathbf{H}_i| = \sqrt{(\mathbf{PH}_i - \mathbf{PH}_j)^2}. \tag{93}$$

$\mathbf{PH}_k$ ($k = i$ or j) is given by

$$\mathbf{PH}_k = r({}^0\mathbf{R}_3{}^3\hat{\mathbf{w}}_k + {}^0\mathbf{R}_G{}^G\hat{\mathbf{v}}_k) = r\mathbf{u}_k. \tag{94}$$

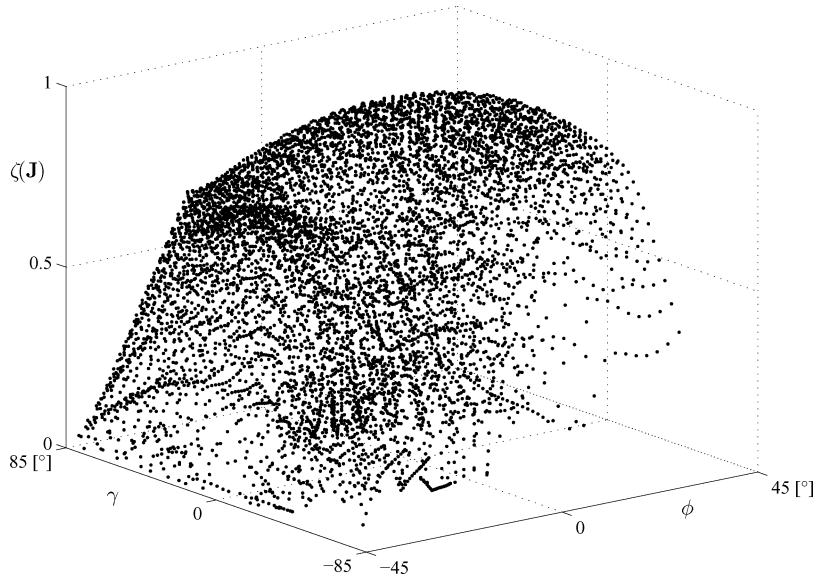


Fig. 7. $\zeta(\mathbf{J})$ vs. γ, ϕ.

https://doi.org/10.1017/S0263574709990683 Published online by Cambridge University Press

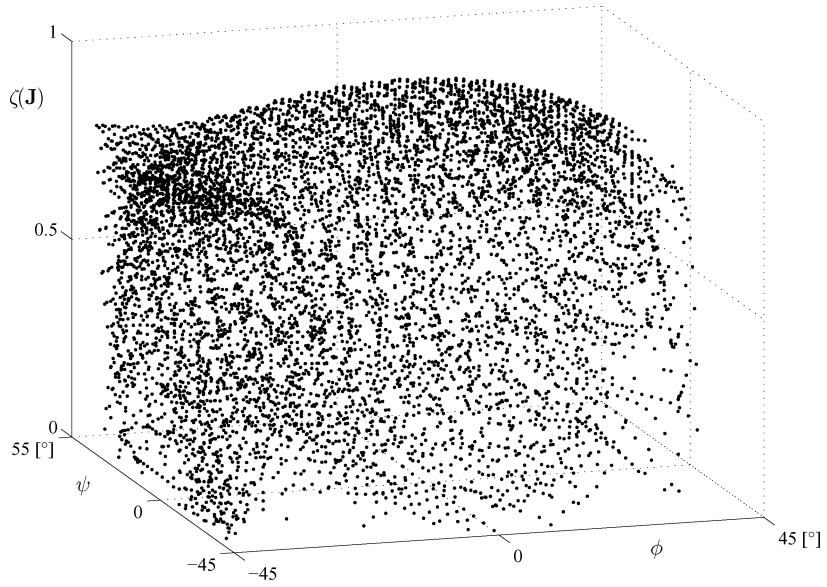


Fig. 8. $\zeta(\mathbf{J})$ vs. ψ, ϕ.

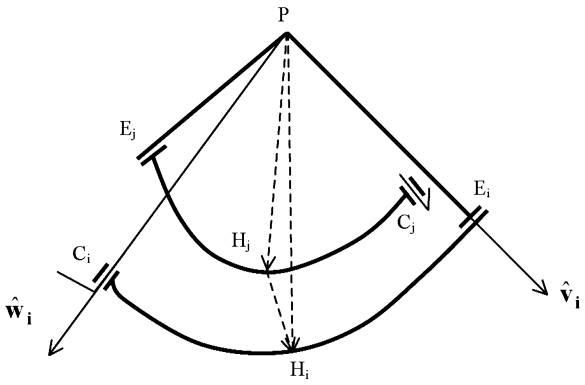


Fig. 9. Mechanical interference geometry.

Thus by introducing Eq. (94) into Eq. (93) the interference condition can be expressed as

$$|\mathbf{H}_j\mathbf{H}_i| = \sqrt{\mathbf{u}_j{}^2 + \mathbf{u}_i{}^2 - 2\mathbf{u}_j \cdot \mathbf{u}_i} = 0. \qquad (95)$$

Terms of Eq. (95) depend on ϑ_{1i} and on Euler's angles. They can be calculated during the motion of the wrist.

Calculation of Eq. (95) was carried out in the case of the numerical example presented in Section 6. Equation (95) is evaluated for each couple of legs at each step of the motion. Calculation is straightforward as $\mathbf{u}_k$ in Eq. (94) is known from the previous kinematics calculations. In the example, distance $|\mathbf{H}_j\mathbf{H}_i|$ is found to be always greater than 0.2 [l.u.] thus guaranteeing that no interference amongst the legs may occur.

10. Conclusion

The paper proposes a detailed analysis of the kinematics of a 3-RRUR manipulator.

The inverse kinematics has 4 solutions for each actuated rotation $\vartheta_{1i} (i = 1, 2, 3)$, the direct kinematics has 32 distinct solutions at most. Investigation on the jacobian proved that both direct and inverse kinematic singularities may theoretically occur. Direct singularities may occur when $\hat{\mathbf{w}}_i$ $(i = 1, 2, 3)$ are coplanar. Instead, inverse singularities may occur whenever, for a leg, the first and last R pair axes are aligned or at least one of the legs is fully folded or stretched.

An example of numerical calculation of the workspace is carried out setting $a = d = 1/2b$. The workspace is obtained by solving the direct position analysis by an iterative procedure starting from the nominal pose of the manipulator. A wide range of variation is obtained for the Euler's angles: $-45° \leq \phi \leq 35°$, $-45° \leq \psi \leq 50°$, and $-80° \leq \gamma \leq 80°$.

The numerical example is also used to inspect on the isotropy and singularities of the manipulator. It is found that the manipulator is isotropic at the nominal pose for which $\phi = \gamma = \psi = 0$. About 35% of orientations reached by the moving platform have $\zeta(\mathbf{J})$ greater than 0.75, thus indicating configurations close to the isotropy. About 20% of orientations give $\zeta(\mathbf{J})$ lower than 0.25, thus indicating a manipulator behavior far from isotropy. One percent of these orientations give $\zeta(\mathbf{J})$ lower than 0.01, thus indicating configurations close to singularities.

In the paper, the geometrical condition for mechanical interference amongst legs is set whenever the last link of each leg is shaped as a circular arc. In the numerical example proposed, the three geometrical conditions are calculated but no mechanical interferences are found.

A deep understanding of kinematic issues, the interesting results obtained in terms of singularities, workspace and isotropy may encourage the authors to develop, as the scope of a future work, a dynamic model of the manipulator and build a hardware prototype.

Acknowledgments

This research was funded by the Italian Ministry of Research (MIUR).

References

1. C. Gosselin and J. Angeles, "The optimum kinematics design of a spherical three-degree-of freedom parallel maipulator," *J. Mech. Transm. Autom. Des.* **111**, 202–207 (1989).

https://doi.org/10.1017/S0263574709990683 Published online by Cambridge University Press

2. L. Birglen, C. M. Gosselin and N. Pouliot, "ShaDe, a new 3-DOF haptic device," *IEEE Trans. Robot. Autom.* **18**(2), 166–174 (2002).
3. C. M. Gosselin, J. Sefrioui and M. J. Richard, "On the direct kinematics of spherical three-degree-of-freedom parallel manipulators of general architecture," *J. Mech. Des.* **116**, 594–598 (1994).
4. C. M. Gosselin and J. F. Hamel, "The agile eye: A high-performance three-degree-of-freedom camera-orienting device", *Proceedings of the IEEE Int. Conf. on Robotics and Automation*, (1994) pp.781–786.
5. C. M. Gosselin and E. Lavoie, "On the kinematic design of spherical three-degree-of freedom parallel manipulators," *Int. J. Robot. Res.* **12**(4), 394–402 (1993).
6. M. Karouia and J. M. Hervé, "A Three-DOF Tripod for Generating Spherical Rotation," In: Advances in Robot Kinematics (J. Lenarcic and M. M. Stanisic eds. Kluwer Academic Publishers, Dordrect, The Netherlands, 2000), pp. 395-402.
7. M. Karouia and J. M. Hervé, "A Family of Novel Orientational 3-DOF Parallel Robots," *Proceedings of RoManSy 14*, Udine (Springer ed., Heidelberg, 2002), pp. 359–368.
8. R. Di Gregorio, "The 3-RRS wrist: A new, simple and non-overconstrained spherical parallel manipulator," *J. Mech. Des.* **126**, 850–855 (2004).
9. R. Di Gregorio, "A new parallel wrist using only revolute pairs: The 3-RUU wrist," *Robotica* **19**, 305–309 (2001).
10. R. Di Gregorio, "Kinematics of a new spherical parallel manipulator with three equal legs: The 3-UCR wrist," *J. Robot. Syst.* **18**(5), 213–219 (2001).
11. X. Kong and C. M. Gosselin, "Type synthesis of 3-DoF spherical parallel manipulators based on screw theory," *J. Mech. Des.* **126**(1), 101–109 (2004).
12. X. Kong and C. M. Gosselin, "Type synthesis of three-degree-of-freedom spherical parallel manipulators," *Int. J. Robot. Res.* **23**(3), 237–245 (2004).
13. X. Kong and C. M. Gosselin, *Type Synthesis of Parallel Mechanisms* (Springer-Verlag, Berlin Heidelberg, 2007).
14. J. J. Craig, *Introduction to Robotics, Mechanics and Control* (Addison-Welsey Publishing Company, Inc., Reading-Massachusetts, USA, 1989).
15. X. Kong and C. M. Gosselin, "Type synthesis of six-DOF wrist-partitioned parallel manipulators," *J. Mech. Des.* **130**(6), 1–8 (2008).

https://doi.org/10.1017/S0263574709990683 Published online by Cambridge University Press